Sensors and Materials, Vol. 30, No. 7 (2018) 1533–1538
MYU Tokyo

S & M 1608

Relationship between Near-infrared Emission of Bi-doped Glass and Preparation Conditions

Hirokazu Masai,[1*] Takenobu Suzuki,[2] and Yasutake Ohishi[2]

[1]National Institute of Advanced Industrial Science and Technology,
1-8-31 Midorigaoka, Ikeda, Osaka 563-8577, Japan
[2] Future-industry Oriented Basic Science and Materials, Toyota Technological Institute,
2-12-1 Hisakata, Tempaku, Nagoya 468-8511, Japan

(Received January 22, 2018; accepted March 27, 2018)

Keywords: glass, emission, near infrared, bismuth

We have examined the effects of Bi concentration, annealing in air, and addition of reducing agent on the near-infrared (NIR) emission of Bi-doped TiO_2–ZnO–B_2O_3–Al_2O_3 (TZBA) glass. Since the decay constants of the NIR emission are independent of the Bi concentration and the preparation conditions, it is expected that a small part of Bi species can act as effective activators in the glass. Annealing affects the blue shift and broadening of the NIR emission. The change in the bandwidth upon Bi or AlN addition can be explained from the viewpoint of the viscosity of the glass melt, which seems to be one of the important factors for obtaining broadband-emitting materials.

1. Introduction

Recently, Bi-containing glass has attracted attention as an optical functional material because of its unique characteristics. In particular, broad emission in the near-infrared (NIR) region is one of the recent attractive characteristics of Bi glass for a wavelength division multiplex system.[1–11] Although the origin of the broad NIR emission of Bi-containing glass is still under discussion, because of the variety of Bi species, such as Bi_2,[12] BiO,[13] and Bi^{2-},[12] such Bi-containing glasses exhibiting broadband emission are promising candidates for super-broadband amplification gain media.

Our group previously reported the NIR emission in CaO–B_2O_3–Bi_2O_3–Al_2O_3–TiO_2 (CaBBAT) glass.[14] Since the activation energy of the NIR emission and that of the electron spin resonance signal in CaBBAT glass show similar values, it is strongly suggested that NIR emission correlates with Bi radical species possessing low valence states. Considering the energy diagram of Bi-related species,[12,13] we assume that the reducing condition during melting is preferable for obtaining better emitting glasses.

To examine the effects of various factors on NIR emission, three factors are chosen. The first is Bi concentration, because there is no clear data on concentration quenching of NIR

*Corresponding author: e-mail: hirokazu.masai@aist.go.jp
http://dx.doi.org/10.18494/SAM.2018.1924

ISSN 0914-4935
http://myukk.org/

emission for the various Bi-doped glasses. The second is annealing in air, because annealing in air may induce both the structural rearrangement of the glass network and the oxidation of Bi activators, whose valence states are conventionally thought to be lower than that of Bi(III).[11–14] The third is the addition of a reducing agent, AlN, because it is thought that a reducing condition is favorable for NIR emission and the addition of AlN can induce a strong reducing atmosphere that can induce the precipitation of Bi nanoparticles during melting.[15] Since the Bi concentration is a changeable parameter in the study, a TiO_2-ZnO-B_2O_3-Al_2O_3 (TZBA) system,[16] which exhibits similar physical properties and crystallization behavior to those of CaBBAT glass, is selected as the host glass. In this study, we discuss several important factors regarding NIR emission of Bi species from the spectroscopic viewpoint.

2. Experimental Procedure

2.1 Preparation of Bi-doped oxide glasses

Bi-doped TZBA glasses were prepared by a conventional melt-quenching method.[16] Batches consisted of TiO_2 (15 mol%), ZnO (25 mol%), B_2O_3 (60 mol%), and Bi_2O_3. The Bi concentrations were 1–5 mol%, which were added as an additional amount. These chemicals were mixed and melted in an alumina crucible in an electric furnace at 1350 °C for 40 min in air. Some samples were added additional AlN (5 mol%) as reducing agents. Since AlN strongly reacts with Pt crucibles, alumina crucibles are suitable for the present examination. The glass melt was quenched on a steel plate at 200 °C, and then annealed at the glass transition temperature T_g (approximately 570 °C) for 60 min. After annealing, the glass samples were cut 10 × 10 × ≈1 mm^3 in size and mechanically polished to obtain a mirror surface. In addition, we have also prepared an annealed sample in order to discuss the effect of annealing in air on the emission property. The annealing was done at T_g + 30 °C for 5 h in air, at which the crystallization of TiO_2 was observed in a previous study.[16]

2.2 Analytical methods

XRD measurements were performed using Ultima IV (Rigaku). Bulk glass samples were excited with a Ti^{3+}:sapphire laser (Coherent, 890) with the wavelength of 800 nm and the laser power of approximately 70 mW. The emission measurement was mechanically chopped at 107 Hz. Emission from the samples was dispersed by a single monochromator [CT-25 (JASCO), blaze wavelength, 1.0 nm; grating, 600 grooves/mm] and detected using a photomultiplier (Hamamatsu Photonics, H10330A-75) with a long-path filter of 800 nm. The emission lifetime $\tau_{1/e}$ of the TZBA glasses was defined as the first e-folding time of the decay curves, detected using a digital oscilloscope (Yokogawa, DL-1640). The absorption spectra were measured within the wavelength range from 300 to 850 nm using a spectrometer (Shimadzu, UV-3150).

3. Results and Discussion

Figure 1(a) shows the optical absorption spectra of the Bi-doped TZBA glasses. The inset shows the enlarged spectra of the Bi-doped glass in the visible region. The absorption band at 2.6 eV, attributed to the absorption of Bi species,[14] increases with increasing Bi concentration. By chemical analysis, the Al_2O_3 amount eluted from the crucible was estimated to be approximately 20 mol%. Figure 1(b) shows the XRD patterns of Bi-doped TZBA glasses after annealing at T_g + 30 °C for 5 h. It is notable that these Bi-containing glasses exhibit no clear diffraction peak attributable to the TiO_2 phase, although similar glasses without Bi addition exhibited precipitation of TiO_2 after a similar heat treatment.[16] Therefore, we assume that the addition of Bi increases the thermal stability of these glasses against crystallization. For practical application, annealing without the precipitation of crystallites is important, because the precipitation of crystallites increases the propagation loss due to the scattering at the interface. Since there was no linear relationship between the NIR emission intensities and the Bi concentrations, we here mainly focus on the spectral shapes. By comparison with the data in the previous report,[11] we can roughly estimate the quantum efficiency of the Bi-doped glasses. From the NIR intensity, it is speculated that the efficiency is approximately 10%. The ambiguity of the Bi concentration dependence suggests that a small number of Bi cations can work as an activator, i.e., not all Bi cations work as activators of the NIR emission.

Figure 2(a) shows the normalized NIR emission spectra of Bi-doped TZAB as-prepared glasses (dashed lines) and annealed glasses (solid lines) obtained by excitation with the wavelength of 800 nm. We observe asymmetric broad emission bands in the NIR region, suggesting the existence of (1) different coordination sites of a Bi species and/or (2) different Bi species. The deviation from the Gaussian peak is observed at the higher photon energy, and most of the emission spectra at least three components. Figure 2(b) shows the emission peak energy and bandwidth (half-width at half-maximum) of NIR emission in Bi-doped TZAB glasses as a function of Bi concentration. These parameters are estimated by Gaussian peak fitting at the normalized intensity region of 0.5–1.0. Although no significant differences

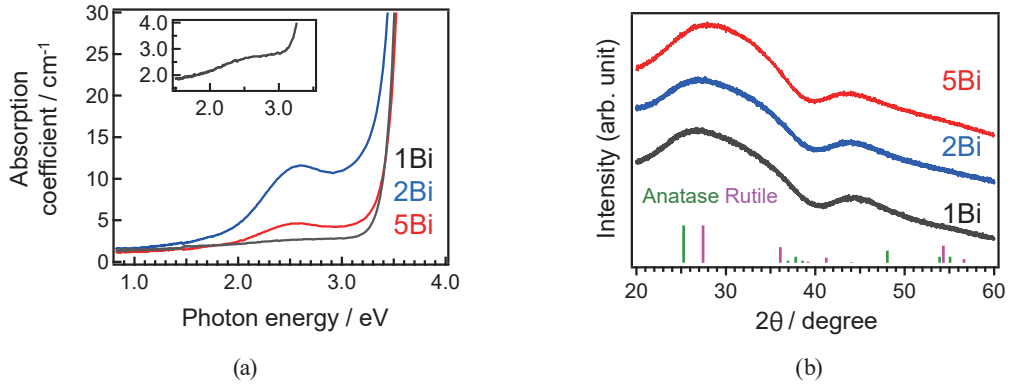

Fig. 1. (Color online) (a) Optical absorption spectra of Bi-doped TZAB as-prepared glasses. The inset shows the enlarged spectra of Bi-doped glass in the visible region. (b) XRD patterns of Bi-doped TZAB glass annealed at T_g + 30 °C for 5 h, along with diffractions of anatase and rutile.

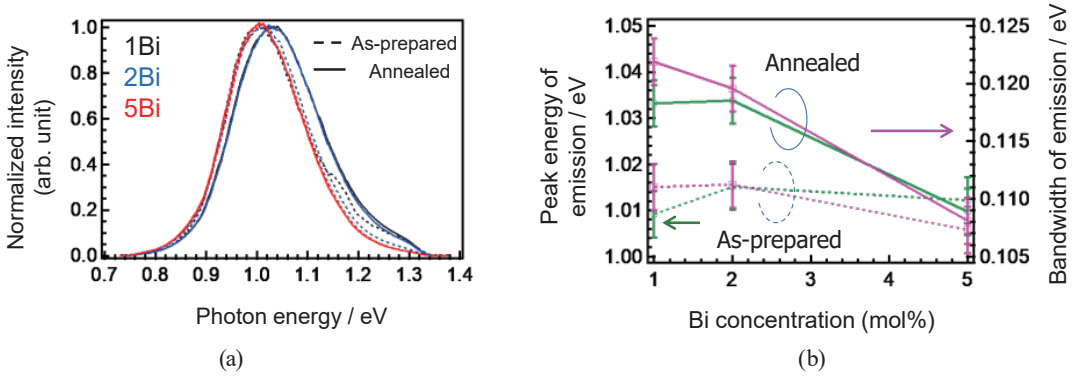

Fig. 2. (Color online) NIR emission of Bi-doped TZAB as-prepared and annealed glasses. (a) PL spectra of Bi-doped TZAB glasses excited with the wavelength of 800 nm. (b) Peak energy and width of emission in Bi-doped TZAB glasses as a function of Bi concentration. The dashed and solid lines correspond to the as-prepared and annealed samples, respectively.

between the two parameters are observed among as-prepared glasses, a slight redshift of the emission peak and the narrowing of the emission bandwidth are observed in annealed glasses with increasing Bi concentration. In addition, after annealing, a blue shift of the emission peak and a broadening of the bandwidth are observed. Since Bi_2O_3 is a low-melting metal oxide, the viscosity of the glass melt is expected to decrease with increasing Bi concentration. Such lower viscosity can induce structural arrangement during the quenching process, which may be one cause of the narrowing of the emission bandwidth. Although the annealing process did not induce the crystallization of TiO_2 nanocrystallites, we assume that other emission sites located at higher peak energies were generated during the heat treatment.

The emission decay curves of Bi-doped TZAB as-prepared and annealed glasses are shown on a linear scale in Fig. 3(a) and on a logarithmic scale in Fig. 3(b). These decay curves take similar decay shapes independent of the Bi concentration and annealing process. As shown in Fig. 3(b), these decay curves are nonexponential, indicating that several activator sites are correlated with the emission, which is consistent with our prediction mentioned above. Table 1 shows the emission decay constant $\tau_{1/e}$ of Bi-doped TZBA glasses. Considering the error bars of the measurements, we assume that these values are within the error bars, and no significant decrease in $\tau_{1/e}$ owing to concentration quenching is observed. It also indicates that the concentration of Bi species, which can act as effective NIR emission centers, is independent of the additional Bi_2O_3 fraction in this concentration range. The idea that some Bi acts as effective emission centers will be adaptable in the $Bi_4Ge_3O_{12}$ scintillator, in which Bi^{3+} species act as emission centers.[17]

Next, we examined another relationship between the addition of AlN and the NIR emission properties of the Bi-doped glasses. Figure 4(a) shows the NIR emissions of AlN, Bi codoped TZAB as-prepared and annealed glasses excited with the wavelength of 800 nm. Although the spectral shapes are similar to those of AlN nondoped samples, the blue shift of the emission peak, which is also observed in nondoped samples, is observed. Similarly to Fig. 2(b), the emission peak energy and bandwidth of the glasses are plotted in Fig. 4(b). Although the relationships with Bi concentration and annealing are similar to those of AlN

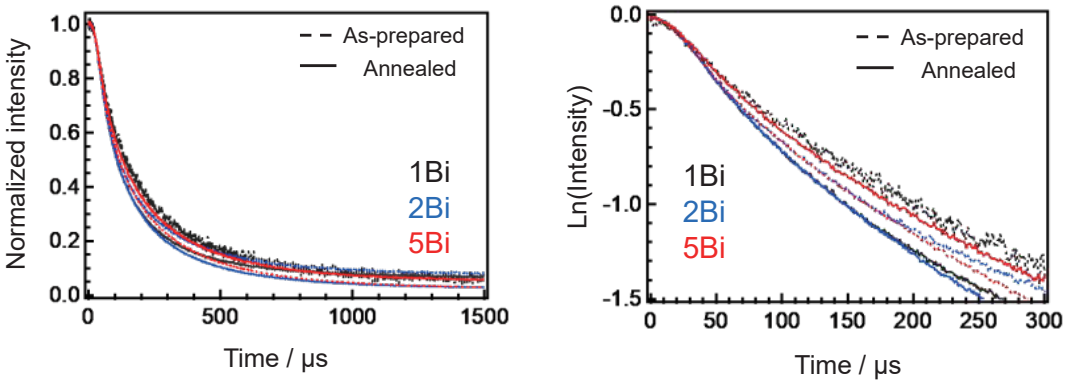

(a) (b)

Fig. 3. (Color online) Emission decay curves of Bi-doped TZAB as-prepared and annealed glasses. The dashed and solid lines represent the as-prepared and annealed samples, respectively.

Table 1
Emission decay constant $\tau_{1/e}$ of Bi-doped TZBA glasses. The error bars are ±20 μs.

	1Bi-TZBA	2Bi-TZBA	5Bi-TZBA
As-prepared	180	150	160
Annealed	150	150	170

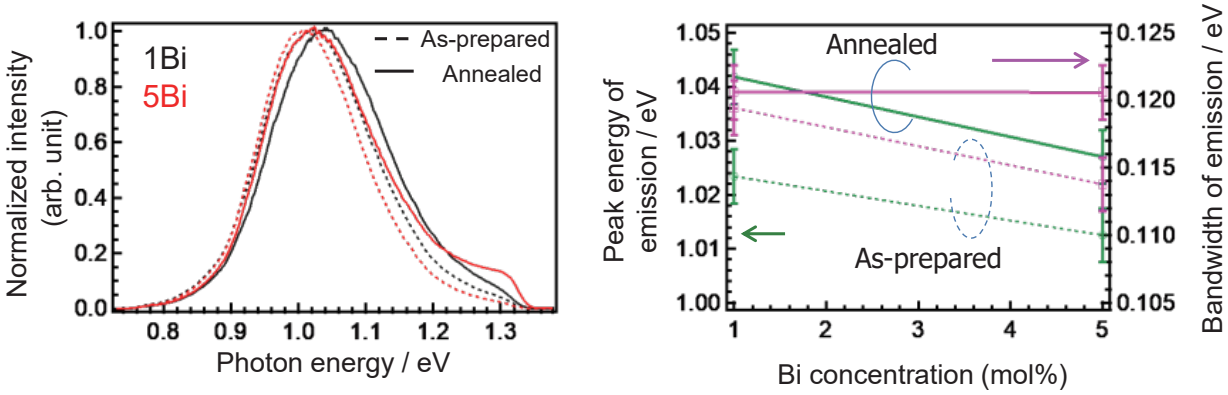

(a) (b)

Fig. 4. (Color online) NIR emissions of AlN, Bi codoped TZAB as-prepared and annealed glasses. (a) PL spectra of Bi-doped TZAB glasses excited with the wavelength of 800 nm. (b) Peak energy and width of emission in Bi-doped TZAB glasses as functions of Bi concentration. The dashed and solid lines represent the as-prepared and annealed samples, respectively.

nondoped glasses, both the peak energy and the bandwidth are slightly larger than those of the nondoped glasses. Since the NIR emission intensities and decay constants are within the error bars, the addition of AlN is not effective for the marked improvement of luminescent performance, i.e., the local coordination state of the activators. Here, we discuss the cause of the broadening of the emission band. During melting, an oxidation reaction from AlN to Al_2O_3 is expected to occur. The generated Al_2O_3 increases the viscosity of the melt, which prevents the structural arrangement during the quenching process. The addition of AlN, therefore,

induces the broadening of the bandwidth in contrast to increasing the Bi_2O_3 concentration. From these results, we believe that Al_2O_3 or a metal oxide, which induces the high viscosity of the glass melt, is effective for broadening the emission. We have reported a relationship between different quenching conditions and the luminescence properties of glasses[18–20] and emphasized that the cooling process from the supercooled liquid state should be affected by the local coordination state of activators. Compared with the previous glass systems,[18–20] the present glass is stronger (viscosity changes slowly above T_g). The present results suggest that the viscosity of the glass melt is important for understanding not only the NIR emission of Bi-containing materials but also other emitting solid-state matters.

4. Conclusions

We examined the effect of the preparation conditions on the NIR emission of Bi-doped oxide glasses. The Bi concentration, the annealing process, and the addition of AlN affect the NIR emission of the glasses. No concentration quenching of NIR emission was observed in the 5Bi-doped TZBA glass, and the relationship between the NIR emission intensity and the Bi concentration is unclear. These results indicate that the concentration of Bi emission centers for NIR emission is much lower than 1 mol%, and their local coordination states are affected by the chemical composition.

Acknowledgments

This work was partially supported by a Grant-in-Aid for Young Scientists (A) 26709048, and the Cooperative Research Project of the Research Institute of Electronics, Shizuoka University.

References

1 Y. Fujimoto and M. Nakatsuka: Jpn. J. Appl. Phys. **40** (2001) L279.
2 Y. Fujimoto and M. Nakatsuka: Appl. Phys. Lett. **82** (2003) 3325.
3 S. Zhou, H. Dong, H. Zeng, G. Feng, H. Yang, B. Zhu, and J. Qiu: Appl. Phys. Lett. **82** (2003) 3325.
4 M. Peng, J. Qiu, D. Chen, X. Meng, and C. Zhu: Opt. Lett. **30** (2005) 2433.
5 X. Meng, J. Qiu, M. Peng, D. Chen, Q. Zhao, X. Jiang, and C. Zhu: Opt. Express **13** (2005) 1628.
6 T. Suzuki and Y. Ohishi: Appl. Phy. Lett. **88** (2006) 191912.
7 H.-P. Xia and X-J. Wang: Appl. Phys. Lett. **89** (2006) 051917.
8 Y. Arai, T. Suzuki, and Y. Ohishi: Appl. Phy. Lett. **90** (2007) 261110.
9 B. Denker, B. Galagan, V. Osiko, S. Sverchkov, and E. Dianov: Appl. Phys. B **87** (2007) 135.
10 T. Murata and T. Mouri: J. Non-Cryst. Solids **353** (2007) 2403.
11 M. A. Hughes, T. Suzuki, and Y. Ohishi: Opt. Mater. **32** (2009) 368.
12 K. Balasubramanian and D. W. Liao: J. Chem. Phys. **95** (1991) 3064.
13 A. B. Alekseyev, H.-P. Liebermann, R. J. Buenker, G. Hirsch, and Y. Li: J. Chem. Phys. **100** (1994) 8956.
14 H. Masai, Y. Takahashi, T. Fujiwara, T. Suzuki, and Y. Ohishi: J. Appl. Phys. **106** (2009) 103523.
15 H. Masai, Y. Takahashi, T. Fujiwara, Y. Tokuda, and T. Yoko: J. Appl. Phys. **108** (2010) 023503.
16 H. Masai, K. Hirakawa, K. Yoshida, T. Miyazaki, Y. Takahashi, R. Ihara, and T. Fujiwara: J. Am. Ceram. Soc. **95** (2012) 3138.
17 P. Dorenbos, J. T. M. deHaas, and C. W. E. van Eijk: IEEE Trans. Nucl. Sci. **42** (1995) 2190.
18 H. Masai, A. Koreeda, Y. Fujii, T. Ohkubo, and S. Kohara: Opt. Mater. Express **6** (2016) 1827.
19 H. Masai, T. Yanagida, G. Okada, A. Koreeda, and T. Ohkubo: Sens. Mater. **29** (2017) 1391.
20 A. Torimoto, H. Masai, G. Okada, and T. Yanagida: Sens. Mater. **29** (2017) 1383.